Facies analysis and diagenetic evolution of the Dinantian carbonates in the Dutch subsurface: data and analyses well KTG-01

Report by SCAN

October 2019

Ministerie van Economische Zaken en Klimaat
ebn
TNO
Interreg North-West Europe DGE-ROLLOUT

Facies analysis and diagenetic evolution of the Dinantian carbonates in the Dutch subsurface: data and analyses well KTG-01

Written by:
Mahtab Mozafari[1], Peter Gutteridge[2], Alberto Riva[3], Kees Geel[4], Joanna Garland[2] and Julie Dewit[2]

October 2019

1- Energie Beheer Nederland (EBN), Daalsesingel 1, 3511 SV Utrecht, the Netherlands
2- Cambridge Carbonates Ltd, No. 4 The Courtyard, 707 Warwick Road, Solihull, B91 3DA, UK
3- G.E.Plan Consulting srl, Via L. Ariosto 58, 44121 Ferrara, Italy
4- Geological Survey of the Netherlands (TNO), Princetonlaan 6, 3584 CB Utrecht, the Netherlands

Dit rapport is een product van het SCAN-programma en wordt mogelijk gemaakt door het Ministerie van Economische Zaken en Klimaat

Table of contents

7. Kortgene-01 (KTG-01) 1

7.1 Introduction 1

7.2 Available dataset 2

7.2.1 Logs 2

7.2.2 Cores, sidewall cores and cuttings 3

7.2.3 Thin sections 3

7.2.4 Additional analyses 4

7.3 Stratigraphy 5

7.4 Sedimentology 5

7.4.1 Depositional environment 10

7.5 Biostratigraphy 11

7.6 Sequence stratigraphy 11

7.7 Diagenesis 12

7.7.1 Paragenetic sequence 12

7.7.2 Cathodoluminescence petrography 18

7.7.3 Stable isotopes 21

7.7.4 Fluid inclusion microthermometry 22

7.7.5 Diagenetic sequence in the context of burial/thermal history 24

7.8 Reservoir quality 25

7. Kortgene-01 (KTG-01)

7.1 Introduction

The KTG-01 well is located in southwest Netherlands, close to wells BHG-01 and S05-01 (Figure 7-1 and table 7-1). KTG-01 was drilled in 1982 and plugged and abandoned as a dry well. The well was drilled through the Beveland Member of the Dinantian carbonates (Zeeland Formation), and also encountered the Bollen Claystone, Devonian Banjaard Group – the well Td'd in the Silurian. No seismic tie is available.

Figure 7-1: Map showing all the wells penetrating the Dinantian carbonates. Location of the KTG-01 well is indicated by red dashed circle.

Table 7-1: Table summarizing the KTG-01 well (from www.nlog.nl).

Co-ordinates (x, y in utm31, ed50 format)	558049, 5714031
Lat/Long (°)	51.57329759, 3.83760312
Supplied co-ordinates	47489, 399317 (RD)
Depth in meters referred to :	Rotary Table
Total depth (m, along hole) :	1900
Vertical position of Rotary Table :	7.96 meter relative to NAP
Trajectory shape :	Deviated
Deviation in X-direction :	13.04
Deviation in Y-direction :	130.32
True vertical depth (TVD) in m :	1887.856

7.2 Available dataset

Most of the available data and reports on the KTG-01 well are available on "www.nlog.nl" within the following link:

https://www.nlog.nl/nlog/requestData/nlogp/allBor/metaData.jsp?tableName=BorLocation&id=106507149

The most relevant publications discussing and presenting the data obtained from BHG-01 well are as following:

Carlson, T. (2019). Petrophysical Report of the Dinantian Carbonates in the Dutch Subsurfaceacies analysis and diagenetic evolution of the Dinantian carbonates in the Dutch subsurface. SCAN Report, 26 p. Report downloadable from www.nlog.nl/scan.

NAM (1982). Core analysis KTG-01. 14 p.

NAM (2000). Note on Evaluation of the Carboniferous (Namurian) intervals in wells: WSK-01, MSL-1, ISB-1, STW-1, KTG-1 and BHG-1. 33 p.

Pickard, N. A. H., and Gutteridge, P. (1997). Dinantian depositional systems and exploration potential: offshore and onshore, The Netherlands. Sedimentological study. Cambridge Carbonates report for NAM, 596 p.

Reijmer, J. J., Johan, H., Jaarsma, B., and Boots, R. (2017). Seismic stratigraphy of Dinantian carbonates in the southern Netherlands and northern Belgium. Netherlands Journal of Geosciences, 96, 353-379. https://doi.org/10.1017/njg.2017.33

RGD (1982). Cuttings descriptions.

RGD (1983). Onderzoek monsters NAM-boring Kortgene-1; Kerntrajecten 946.90-995.60, 1351-1365.10, 1720.33-1735 en 1891.50-1900 (4 bijlagen). Rapport no. GB 1888 / OP 9235, 17 p.

7.2.1 Logs

This well has a complete suite of logs and has been petrophysically evaluated within the framework of the SCAN project (Carlson, 2019). Spectral gamma ray is available, and a clay curve has been produced based on the Potassium content (brown colour). Accordingly, there are several intervals in the well where clays are present. The high clay content towards the base of the core represents the ?Devonian clastics interval.

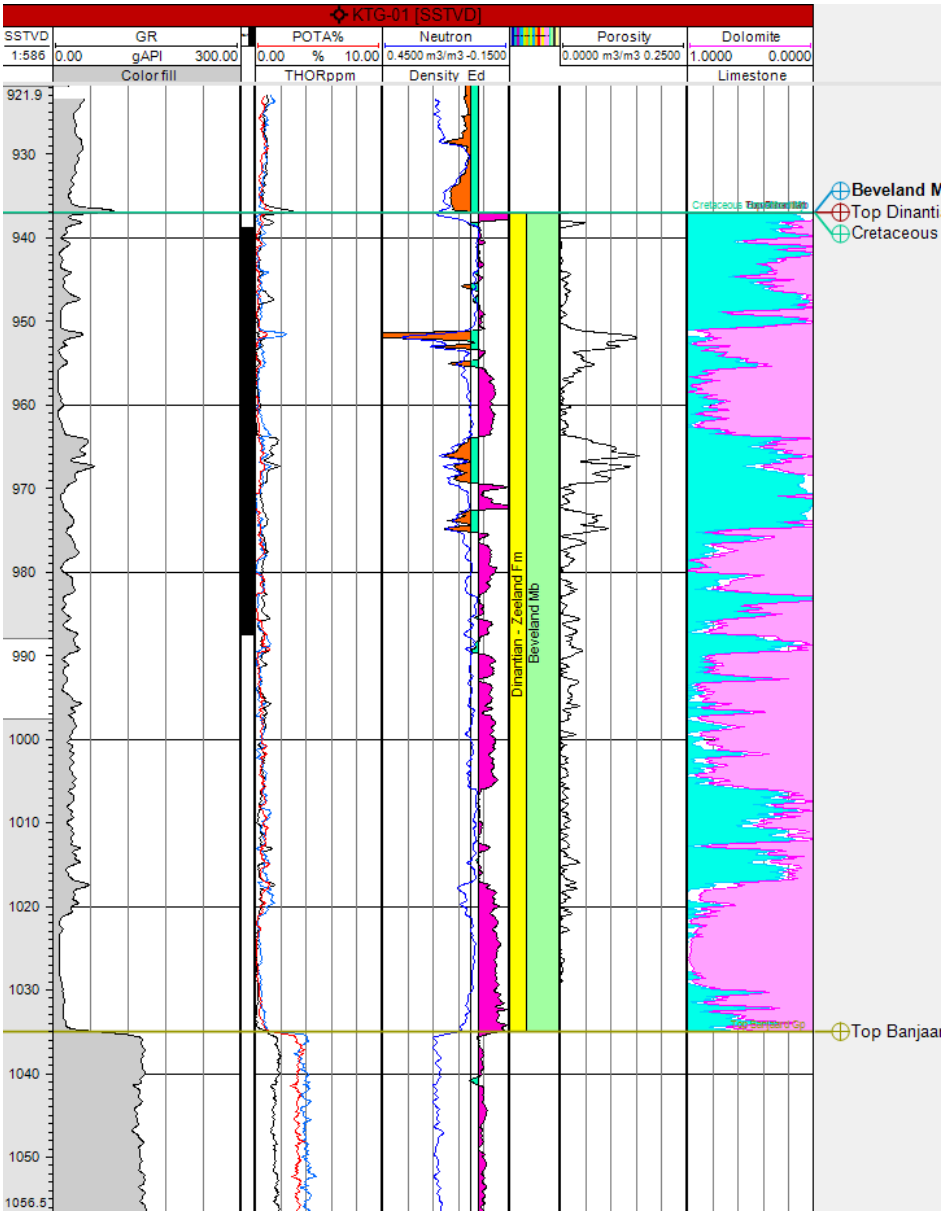

Figure 7-2: Gamma ray, neutron/density, porosity and mineralogical logs in the KTG-01 well.

7.2.2 Cores, sidewall cores and cuttings

Cores 1 to 4 were cut just in the Beveland Member below the base Cretaceous unconformity , in the interval 946.0 m to 996.0 m (50 m).
Cores were also taken in the Devonian Banjaard Group, but these were not evaluated in this study. A total number of 74 Dinantian thin sections were described in the Cambridge Carbonates (1997) report. The majority of these were made available to EBN at NAM core store in Assen (six thin sections were missing), and photomicrographs taken and thin sections scanned. No cuttings were available for the uncored interval. No SWC's are available.

7.2.3 Thin sections

At the NAM core store 64 thin sections were studied. In addition, six samples were selected for further cathodoluminescence petrography (Table 7-2). For these samples new polished thin sections were made.

7.2.4 Additional analyses

The following additional data (Table 7-2) were acquired as part of the SCAN project:

Table 7-2: Overview of the samples selected for the diagenetic study of the KTG-01.

Depth (m)	Sample type	Polished slab/thin section	C and O isotopes (vein)	C and O isotopes (matrix)	C and O isotopes	FI	Biostrat	CL	Analyses	Aims of analyses
951.1	Dolomite vein	1	1	1	X fracture (fill and bulk)	1		1	CL, isotopes, fluid inclusion	Timing and fluids involved in cementation
966.88	Dolomite	1		1	X (bulk)			1	Whole rock stable C and O	Origin of dolomite
967.77	Dolomite with dolomite vein	1	1	1	X fracture (fill and bulk)			1	CL whole rock stable C and O	Timing and fluids involved in cementation
973.65	Limestone			1	X (bulk)				Whole rock stable C and O	Diagenesis
976.15	Limestone with calcite vein and Cretaceous karst fill	1	1	1	X fracture (fill and bulk)			1	CL whole rock stable C and O	Timing and fluids involved in cementation
976.75	Calcite vein and Cretaceous karst fill	1	1	2	X fracture fill, Dinantian bulk and Cretacoeus bulk)	1	1	1	Biostrat, CL, isotopes of bulk and fracture, fluid inclusion	Dating of karst fill, timing and fluids involved in cementation
978.05	Limestone			1	X (bulk)				Whole rock stable C and O	Diagenesis
984.65	Dolomite			1	X fracture (fill and bulk)					
984.65	Dolomite		1		X fracture (fill and bulk)			1	CL	Paragenetic sequence
985.2	Dolomite			1	X (bulk)				Whole rock stable C and O	Diagenesis
985.7	Dolomite			1	X (bulk)				Whole rock stable C and O	Diagenesis
994.55	Dolomite			1	X (bulk)				Whole rock stable C and O	Diagenesis

7.3 Stratigraphy

The succession of the Kortgene-01 well spans from Quaternary to ?Silurian (Table 7-3), encountering the Cretaceous unconformity at 945 m MD above the eroded Dinantian intervals. Only the lowermost parts of the Dinantian were encountered.

Table 7-3: Stratigraphy of the KTG-01 well (from www.nlog.nl).

Stratigraphical unit	**Top interval**	**Base interval**
QUATER. UNDIFF.	0	52
Oosterhout Formation	52	88
Breda Formation	88	101
Rupel Clay Member	101	183
Vessem Member	183	203
Asse Member	203	345
Brussels Sand Member	345	405
Ieper Member	405	603
Basal Dongen Sand Member	603	628
Landen Clay Member	628	678
Ommelanden Formation	678	945
Beveland Member	945	1043
Bollen claystone formation	1043	1350
Banjaard group	1350	1690
Silurian?	1690	1900

7.4 Sedimentology

Cores 1 to 4 were cut just below the Cretaceous unconformity. Evidence of the ?Jurassic to Cretaceous erosion-event is present in the cores through the development of an extensive karst system partly filled by Cretaceous-aged marine sediments. Further cores were cut in the Devonian and ?Silurian, but these were not evaluated for the present study.

Figure 7-3: Overview of the sedimentological log constructed for the KTG-1 well (an image of higher resolution is available in Appendix B).

The basal part of the cored succession (ca. 987.4 - 996.8 m) consists of a series of small-scale cycles (<1 to 3 m thick). Fine-grained peloid-bioclast grainstones form the base of the cycles and are capped by fenestral mudstones and wackestones possessing a limited fauna of ostracodes-calcispheres (Figure 7-4). Evidence for exposure is common with local development of pedogenic features, such as soil peloids, pisoids, roots and calcrete nodules. Similar cycles are also present at the top of the cored interval (946.0 - 955.6 m) where many of the cycle bases are clearly erosive; intraclast-bioclast grainstones overlie irregular erosional surfaces cut into fenestral calcisphere-ostracode wackestones (Figures 7-5 and 7-6). Laminated and thrombolitic algal mats cap some of the cycles (Figures 7-7).

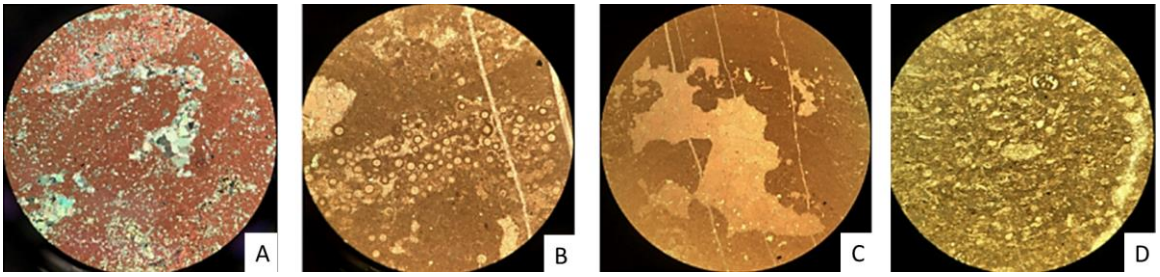

Figure 7-4: Representative photomicrographs of the facies types observed in the KTG-01 well. Fenestral mudstone and wackestone: A) (996.74 m, PPL, FOV 4 mm). B) (995.20 m, PPL, FOV 2 mm). C) (995.20 m, PPL, FOV 4 mm). D) Fine-grained peloid-bioclastic grainstone (992.75 m, PPL, FOV 4 mm).

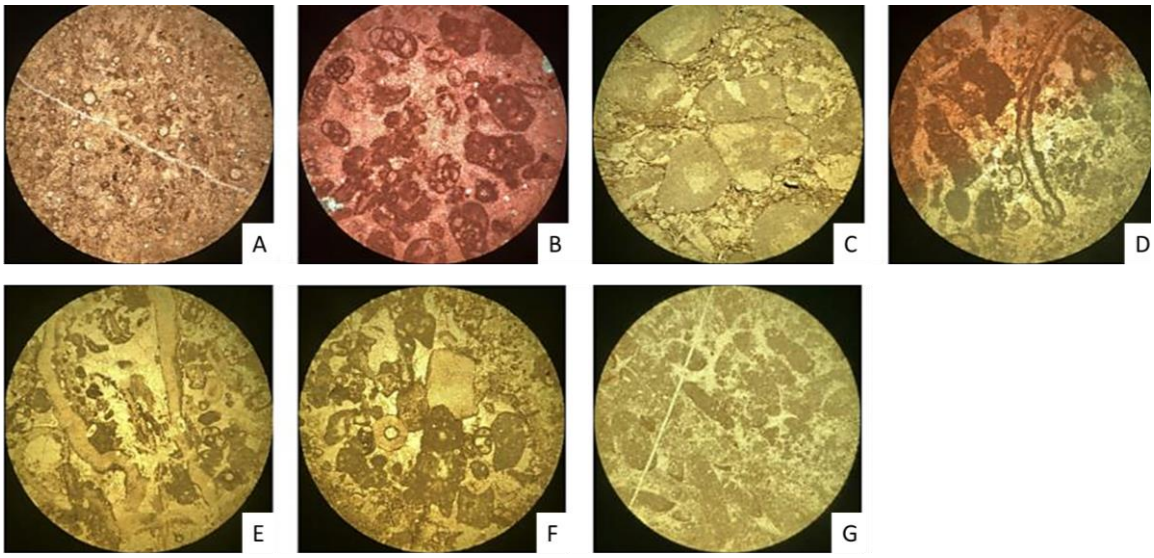

Figure 7-5: Representative photomicrographs of the facies types observed in the KTG-01 well. Intraclast-bioclast grainstone: A) (954.70 m, PPL, FOV 2 mm). B) (955.50 m, PPL, FOV 2 mm). C) (951.40 m, PPL, FOV 2 mm). D) (949.30 m, PPL, FOV 4 mm). E) (948.70 m, PPL, FOV 4 mm). F) (948.70 m, PPL, FOV 4 mm). F) (948.70 m, PPL, FOV 4 mm). G) (946.00 m, PPL, FOV 2 mm).

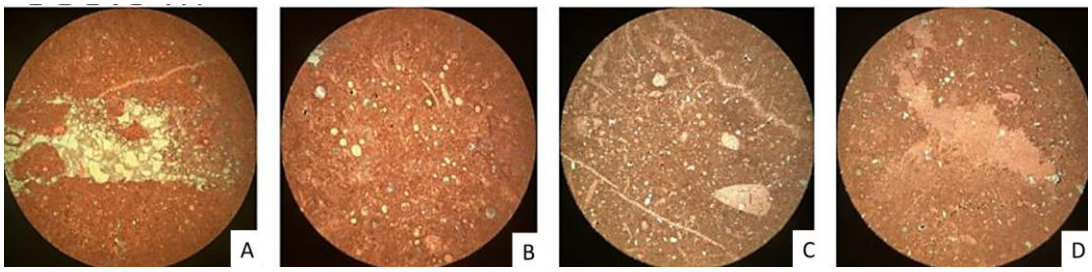

Figure 7-6: Representative photomicrographs of the facies types observed in the KTG-01 well. Fenestral calciphere-ostracode wackestones: A) (952.00 m, PPL, FOV 4 mm). B) (952.00 m, PPL, FOV 2 mm). C) (948.70 m, PPL, FOV 2 mm). D) (948.70 m, PPL, FOV 2 mm).

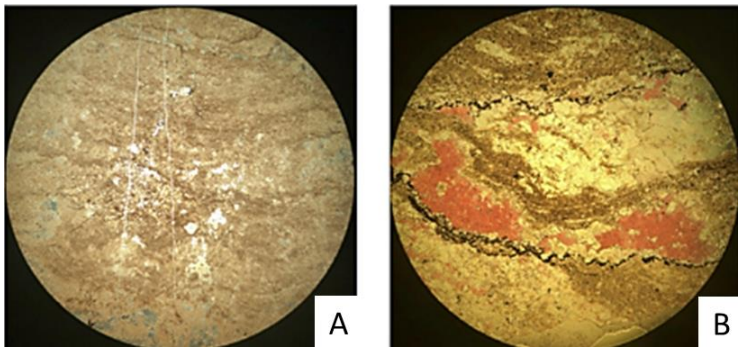

Figure 7-7: Representative photomicrographs of the facies types observed in the KTG-01 well. Laminated and thrombolytic algal mats: A) (946.60 m, PPL, FOV 8 mm). B) (947.80 m, PPL, FOV 4 mm).

Thicker units (ca. 5 to 10 m) of grainstones form the middle part of cored interval (955.6-987.4 m) and also define distinct cycles. Cycle bases are generally marked by heavily compacted bioclastic packstones. Intense compaction has resulted in the development of fitted-fabrics with numerous thin anastomosing pressure dissolution seams, imparting an argillaceous appearance to the limestones (Figure 7-8).

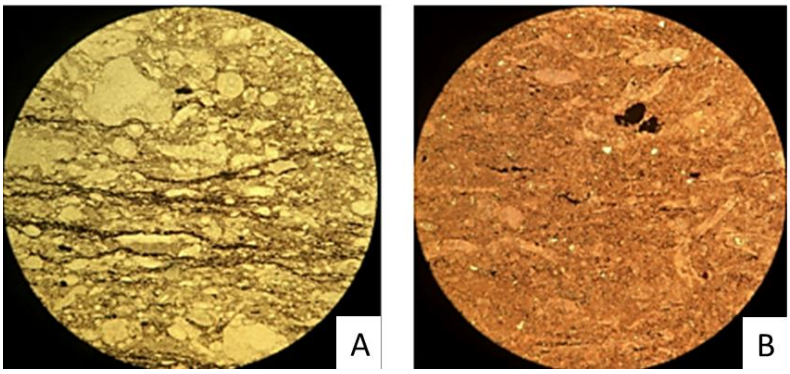

Figure 7-8: Representative photomicrographs of the facies types observed in the KTG-01 well. Bioclastic packstones: A) (973.60 m, PPL, FOV 4 mm). B) (972.40 m, PPL, FOV 4 mm).

The middle and upper part of the cycles are typically massive intraclast-peloid-bioclast grainstones (Figure 7-9) with little or no evidence of compaction. Although intervals of coarse dolomite are common in these cycles (Figure 7-10), ghost fabrics are generally preserved revealing that the former limestones were predominantly peloid-intraclast grainstones. Cycle tops are generally thin in comparison with the underlying grainstones and

typically consist of calcisphere-ostracode wackestone (Figure 7-11) with oncoids and local development of fenestral fabrics. Pedogenic features such as calcrete nodules are normally present at the top of the cycles indicating periods of subaerial exposure.

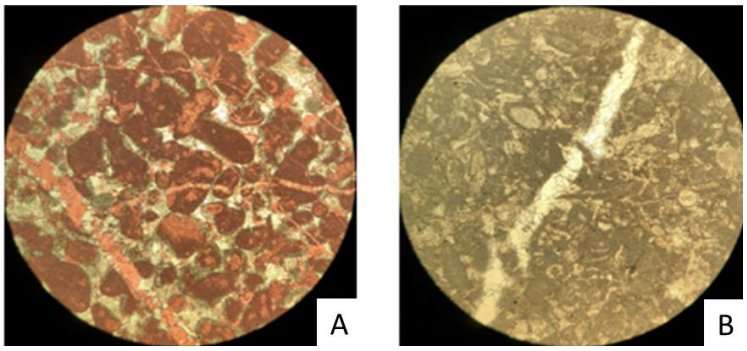

Figure 7-9: Representative photomicrographs of the facies types observed in the KTG-01 well. Intraclast-peloid-bioclast grainstone: A) (962.85 m, PPL, FOV 4 mm). B) (962.85 m, PPL, FOV 4 mm).

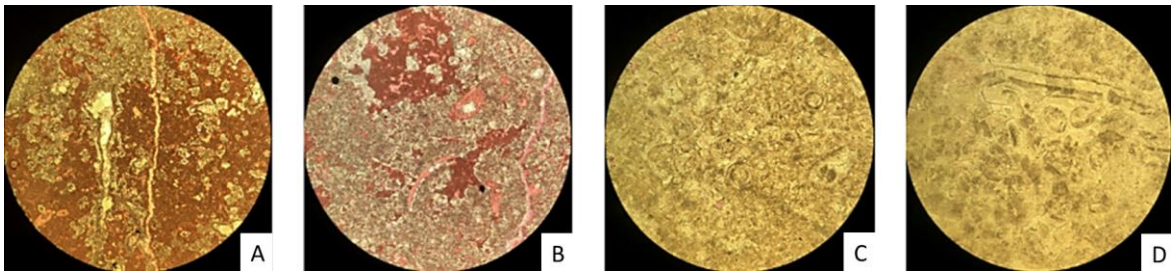

Figure 7-10: Representative photomicrographs of the facies types observed in the KTG-01 well. Dolomitised peloid- intraclast grainstone: A) (974.05 m, PPL, FOV 4 mm). B) (971.20 m, PPL, FOV 2 mm). C) (970.30 m, PPL, FOV 4 mm). D) (969.70 m, PPL, FOV 4 mm).

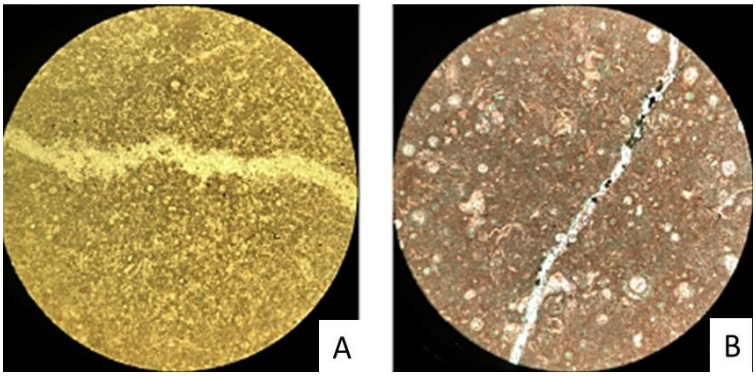

Figure 7-11: Representative photomicrographs of the facies types observed in the KTG-01 well. Fenestral calciphere-ostracode pack- to wackestone: A) (977.70 m, PPL, FOV 4 mm). B) (976.75 m, PPL, FOV 2 mm).

7.4.1 Depositional environment

Shallow subtidal to intertidal deposition is recorded by the facies present in the cored interval. Shallow subtidal sediments are dominated by non-bioclast allochems. Intraclasts of micrite and fine grained bioclastic wackestone indicate extensive erosion and reworking of partially lithified 'muddy lithologies' into subtidal sand shoals. The development of tidal channels in extensive tidal flats could have sourced many of the intraclasts, which were then re-worked into extensive offshore sand shoal systems. The preponderance of palaeoberesellid algal grains in bioclastic component of the sediments suggest deposition in relatively shallow water; palaeoberesellids are generally considered to have preferred a shallow water probably less than ca. 10 m.

Many of the cycles are capped by fine grained bioclastic mudstones and wackestones that possess restricted fauna and fenestral fabrics. The presence of fenestrae is indicative of periodic exposure, probably in an intertidal or supratidal setting. Cycles capped by fenestral micrites illustrate limited progradation of tidal flats on the Tournaisian and early Viséan platforms that bordered the London-Brabant Massif. Moreover, the cycles appear to have been exposed; pedogenic features (soil peloids, pisoids, rhizocretions and nodular calcrete) are commonly developed at the top of the cycles.

The character of the cyclicity varies throughout the cored interval. Small-scale cyclicity is developed at the base and top whereas thicker cycles dominate the middle part of the core. In sequence stratigraphic terms high accommodation rates, such as may be expected during transgressions would enable thick cycles to be deposited whereas low accommodation rates would favour the accumulation of thin cycles. As such the interval cored in KTG-01 can be viewed as two regressive high stand systems (thin subtidal-intertidal cycles) separated by a transgressive system were cycles are dominated by thick subtidal sequences.

One the most striking features of the KTG-01 cores are a series of karstic fractures, vugs and caves filled by various types of sediment and cement. These karstic features are of Dinantian and Cretaceous age.

At least two phases of karstification are represented in the cored interval:

- Intra- or Late-Dinantian karst. Characterised by calcite cemented fractures and fissures with dark clay sediment fill. The fractures have an anastomosing character and locally form a crackle-breccia texture. The fractures vary in thickness over a short distance and are solution-enhanced. In thin section, the Dinantian karst fissures are often lined by coarse, zoned calcite cements.
- The Cretaceous karst fill can be quite varied. Commonly the karst cavities are infilled by sediments rich in glauconite, broken up inoceramids, calcispheres and planktonic foraminifera. These sediments are notably microporous. Laminated micrites and clays are also present locally as fissure fills. Some layers contain irregular and laminar fenestrae that are partly infilled by geopetal calcisiltite. Intraclasts of the host rock are common components, and locally form a breccia texture (e.g. 982 m).

Dating of the karst infill (SCAN project) reveals the following:

KTG-01, 975.95 m: Late Cretaceous. A low abundance, long-ranging foraminiferal assemblage of Late Cretaceous age is recorded, including *Globigerinelloides. asperus*, *Heterohelix globulosa*, *Eponides* spp., with inoceramid debris and sponge spicules.

KTG-01, 976.75 m: Late Cretaceous, Campanian? – Maastrichtian? Very few foraminifera are identified in thin section with rare *Eponides* spp. and single occurrences of *Gavelinella* spp., *G.asperus*, *Stensioeina pommerana*?, with common inoceramid debris also identified. This represents a broad Late Cretaceous microfaunal assemblage, potentially restricted to a Maastrichtian – Campanian age based on the questionable occurrence of *S. pommerana*.

Microscopically, the margins of the fissures are commonly rich in barites and pyrite mineralisation. Neomorphism of clay sediments into large calcite fans are also present.
The Cretaceous karst systems typically occur within dolomitised Dinantian sediments – it is considered that the dolomites had improved permeabilities, and therefore were the focus for meteoric waters. These karst systems commonly exploit pre-existing stylolites.
In many examples a complex fracture and vug network formed, which is cemented by dolomite and saddle dolomite (i.e. at 984.5 m). Vugs locally have a geopetal sediment fill at their base (e.g. 966.15 m and 966.01 m). It cannot be said with certainty which karst system these belong to, as they do not have a fill which is indicative.

7.5 Biostratigraphy

According to Pickard and Gutteridge (1997), the foraminifera associations in Cores 1 to 4 are dated as V1 or older in age (Tournaisian-Moliniacian: Rijks Geologische Dienst, 1983). The absence of archaediscids from the thin sections indicates that the rocks are older than the Cf4b foraminifera-biozone. However, the presence of the dasycladacean alga Koninckopora in samples above 951.4 m shows that the uppermost part of the cored interval belongs to the Eoparastaffella Cf4a Subzone and are thus of V1a, earliest Moliniacian-age.
A thick succession of clastics is present below the cored interval, and there is some confusion relating to the age of these. NLOG suggest that these are Devonian and Silurian clastics, but the RGD (1983) indicates that these are Upper Tournaisian and Middle Devonian in age. This dating, however, is based on comparison with the Belgian Ardennes rather than unequivacable data, so it is not clear which is correct. If there are Tournaisian clastics, then this is important for palaeogeographical purposes.

7.6 Sequence stratigraphy

Two depositional cycles, based on correlations with O18-01, BHG-01, S02-02 and S05-01, have been recognised in KTG-01. A total of ten depositional cycles representing the whole of the Dinantian have been recognised in the SW Netherlands; the lower most two depositional cycles are present in the KTG-01 well (Figure 7-12).
Cycle 1a: This cycle represents the initial flooding of the basin; the thin TST is characterised by a clean gamma interval above the thick high gamma fine clastics at the top of the Tournaisian. This is interpreted as deposition of clean carbonates in shallow water. This is followed by increasing gamma interpreted as deposition of more muddy carbonates in deeper water. The cored interval in KTG-01 represents the HST of this cycle was where is consists of thinly-bedded cyclic inner ramp carbonates with cycle boundaries marked by horizons with calcrete, rhizocretions or peritidal carbonates.
Cycle 1b: This cycle represents the TST, maximum flooding interval and part of the HST which was cored in well KTG-01; this cycle shows an upward transition from thinly bedded wackestone deposited in a deep subtidal setting to thickly bedded cyclic grainstone and packstone with cycle top marked by peritidal facies and rhizocretions. The basal cycle boundary of 1b depositional cycle represents an upward change to thicker, deeper ramp cycles. The cycles above 1b depositional cycle are missing as a result of sub-Cretaceous erosion. The Dinantian carbonates also contain karst cavities infilled by Dinantian allochems; these may represent karst at intra-Dinantian cycle boundaries or karst below the Limburg Group.

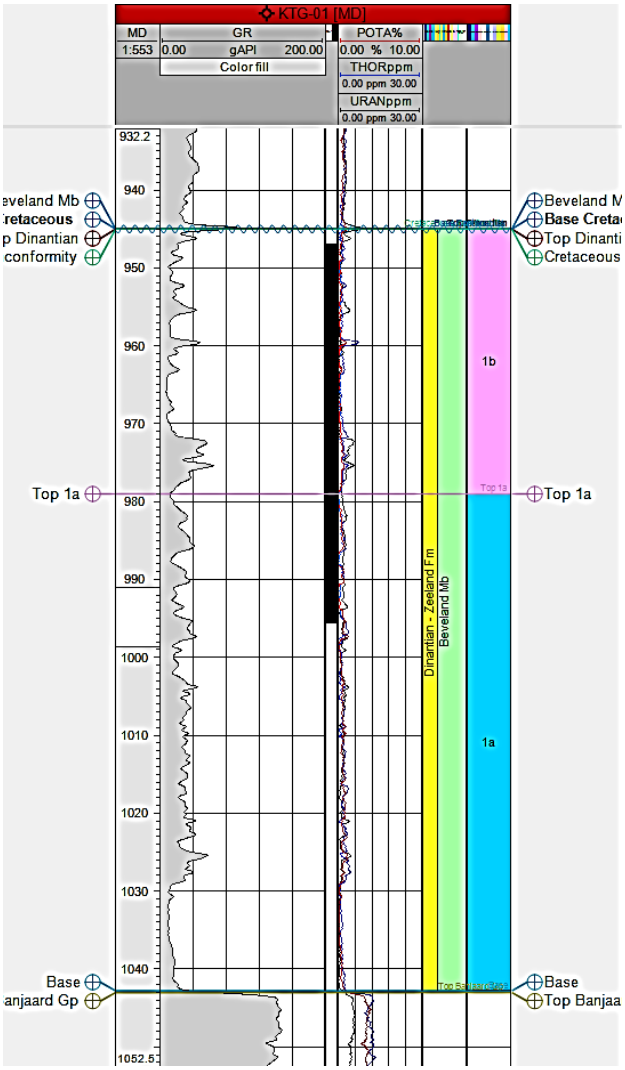

Figure 7-12: Depositional cycles recognised in the KTG-01 well.

7.7 Diagenesis

7.7.1 Paragenetic sequence

Based on the core observations and available thin sections the following paragenetic sequence was established (the main diagenetic phases are illustrated in Figures 7-13 to 7-16):

Eogenesis

1. Grain micritisation and dissolution of aragonite components (Figure 7-5D).
2. Early fenestral vugs associated with intertidal settings (syn-sedimentary)
3. Early (Dinantian) karstification - dissolution/enlargement of pores/fractures (early dissolution). Creation of vugs – geopetal fills of some vugs. Sediment fill of some fissures.

Shallow Burial

4. Calcite cement within interparticle pore space – shallow burial: C1 + C2
5. Dolomitisation and dolomite cements pre-dating compaction: D1

Deeper Burial

6. Chemical compaction
7. Calcite cemented hairline fractures – post-dates early D1 dolomite: C3
8. Replacement dolomite/dolomite cement in vugs and fractures: D2
   Dolomite often concentrated along stylolites.
9. Non-ferroan, poikilotopic calcite cement in vugs: C4
   (not clear if this pre-or postdates Cretaceous karstification at this stage)
10. Pyrite (lining vugs and fractures, associated with C4)
11. Fractures and non-ferroan calcite cement post-dating D2 dolomite: C5
12. Fractures and ferroan calcite cement fill: C6
    Note that for C4 and C5 only cross cutting relations with D2 are observed. These phases may also have formed later.

Telogenesis

13. Cretaceous karst dissolution and sediment fill.
14. Calcite associated with fissure-fil/speleothem: C7

Re-burial

15. Mineralisation of the Cretaceous karst infill:
    - Barites crystals, associated with Cretaceous Karst fill, particularly at margins of fissures
    - Minor non-ferroan dolomite cement: D3
    - Coarse calcite cements associated with Cretaceous karst fill: C8
16. Calcite vein cross cutting the Cretaceous karst fill: C9
17. Authigenic silica
18. Bitumen

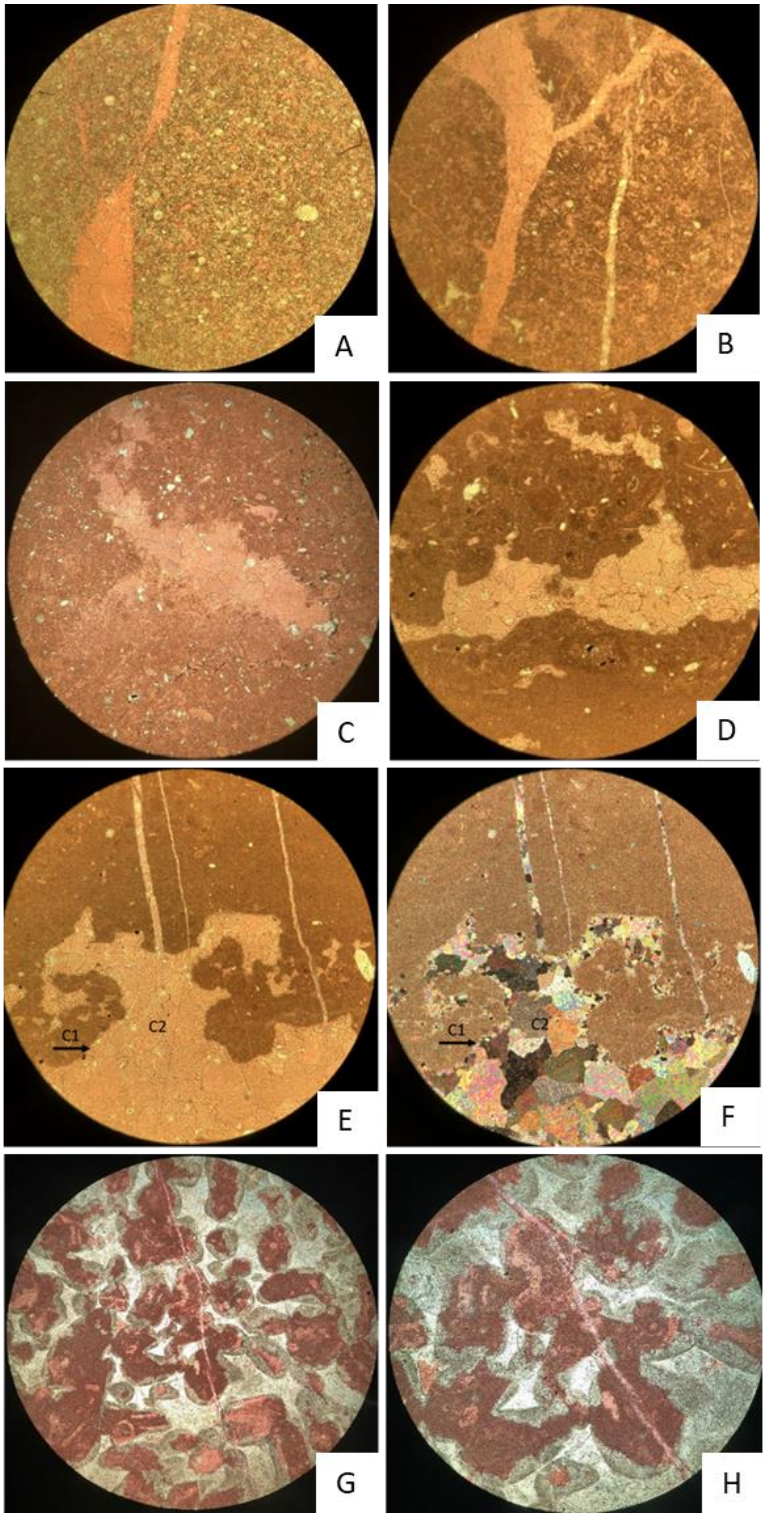

Figure 7-13: A, B) Early fenestrate vugs associated with intertidal settings (syn-sedimentary); (948.70 m, FOV 2 mm), (995.20 m, FOV 2 mm). C, D) Early Dinantian karstification-dissolution/ enlargement of pores/fractures (e.g. 952.0 m; 977.7 m; 992.75 m). Creation of vugs (955.9 m)-geopetal fills of some vugs (955.9 m; 996.74 m). Sediment fill of some fissures (962.8 m; 992.75 m; 996,74 m); (977.70 m, FOV 4 mm), (977.70 m, FOV 4 mm). E, F) Calcite cement (C1+C2) within interparticle pore space-shallow burial. C1 is fine crystalline and fringes pores. C2 is equant calcite occluding pore spaces; (995.20 m, PPL, FOV 2 mm), (995.20 m, XPL, FOV 2mm). G, H) Dolomitisation and dolomite cements pre-dating compaction (D1) + C3 calcite vein cross cutting D1; (961.30 m, FOV 4 mm), (961.30 m, FOV 2 mm).

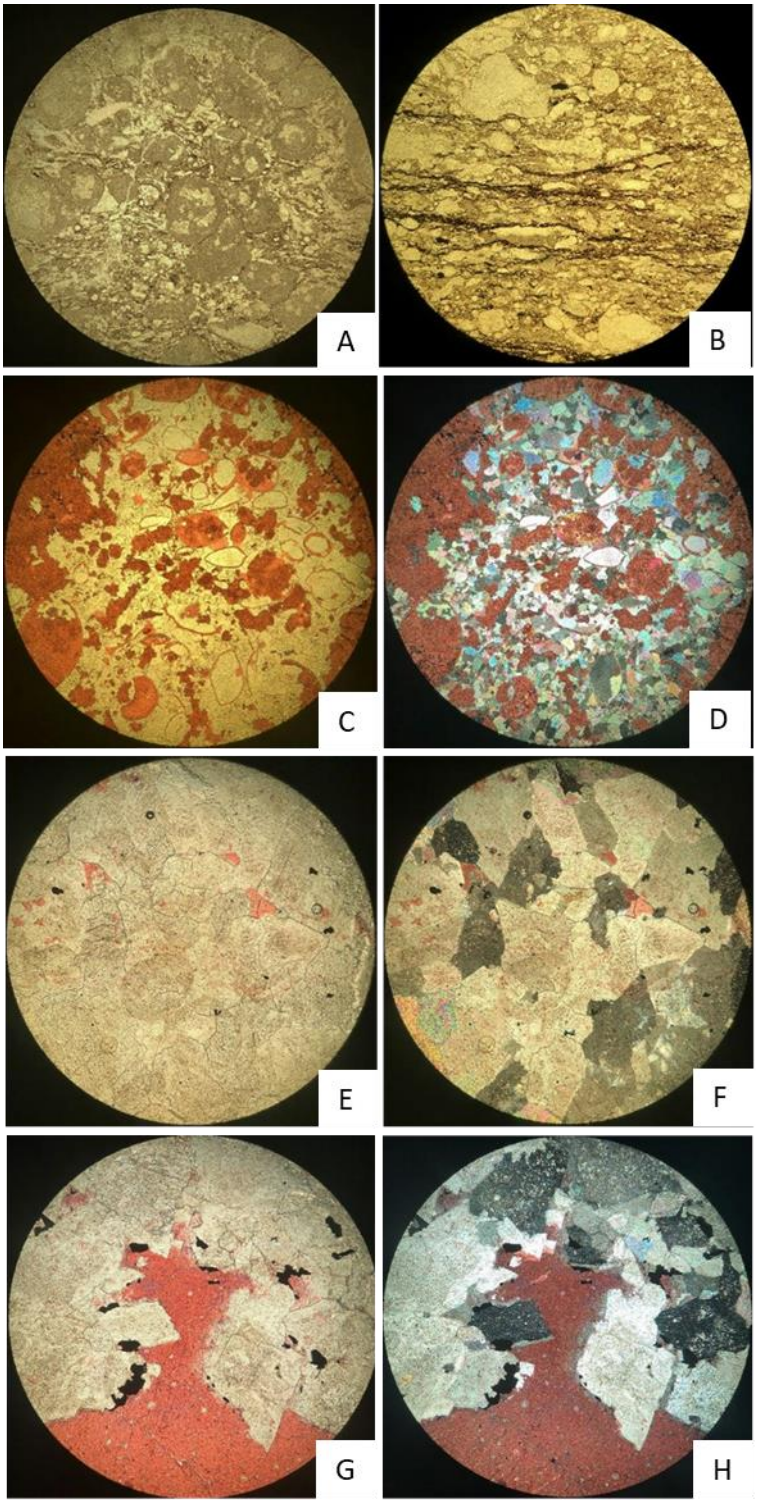

Figure 7-14: A, B) Chemical compaction (951.40 m, FOV 4 mm), (973.60 m, FOV 4 mm). C, D) Replacement dolomites in vugs (946.60 m, PPL and XPL, FOV 4 mm). E, F) D2 dolomite replacing a ooid/intraclastic grainstone (959.0 m, PPL and XPL, FOV 2 mm). G, H) D2 dolomite post-dated by pyrite and calcite cement C4 (959.0 m, PPL, XPL, FOV 2 mm).

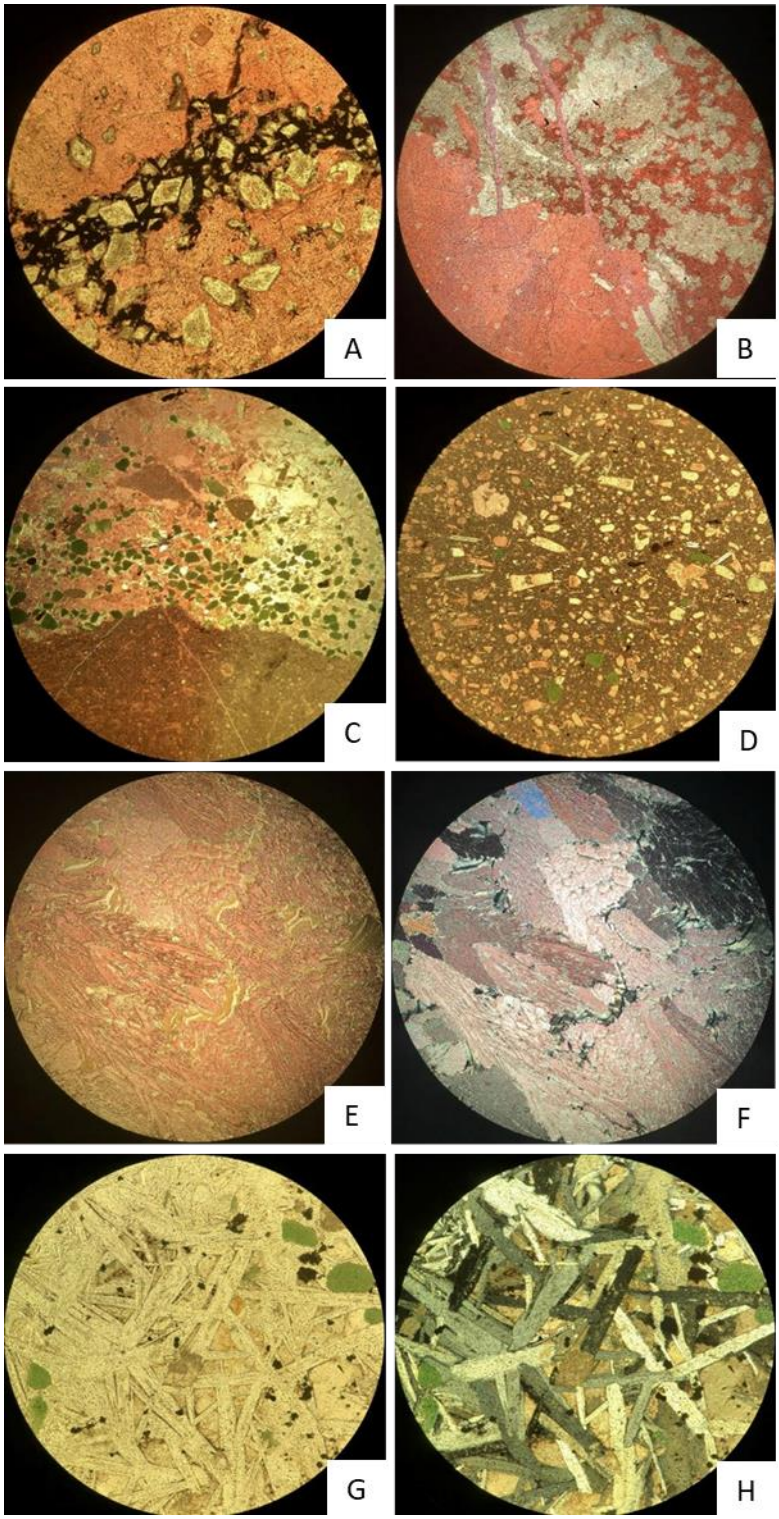

Figure 7-15: A) D2 dolomite concentrated along stylolites (970.10 m, FOV 2 mm). B) Ferroan calcite veins post-dating dolomites (955.90 m, FOV 2 mm). C, D) Cretaceous karst sediment fill (983.76 m, FOV 8 mm), (976.10 m, FOV 4 mm). E, F) Speleothem (960.10 m, PPL and XPL, FOV 4 mm). G, H) Barite precipitation in Cretaceous karst sediment (981.95 m, PPL and XPL, FOV 2 mm).

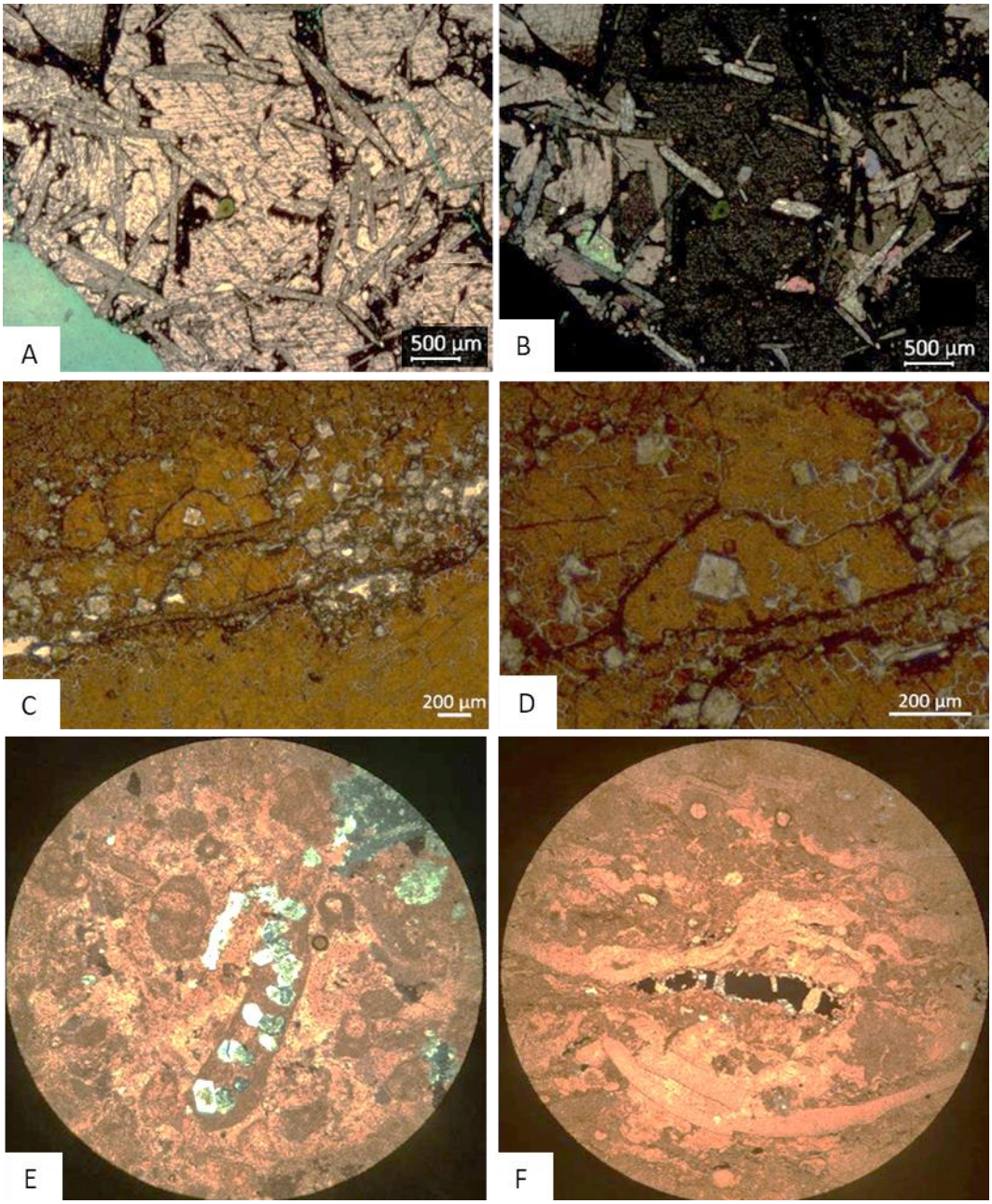

Figure 7-16: A, B) Coarse calcite cement C8 post-dating the mineralisation of the Cretaceous karst infill (976.15 m, PPL and XPL). C, D) D3 associated with C8 and barite mineralisation of the Cretaceous karst infill (976.15 m). E) Autogenic silica (955.5 m, FOV 2 mm). F) Bitumen concentrated within a vug (948.10 m, FOV 2 mm).

7.7.2 Cathodoluminescence petrography

Of the samples selected for further diagenetic analysis four samples consist of dolomite, i.e. 951.10 m, 966.88 m, 967.77 m and 984.65 m, and three samples consist of calcite, i.e. 976.15 m and 976.75 m. The dolomite samples are representative for the D2 dolomite. The calcite sample 976.75 m consists of a calcite vein cross cutting the Cretaceous karst infill (C7). The calcite sample 976.15 m is representative of the C8 calcite associated with the mineralisation of the Cretaceous karst infill.

D2 (+C4): The D2 dolomite is generally dull to non-luminescent (Figures 7-17 A and B). The matrix dolomite is fine crystalline and sub- to anhedral. The dolomite cement is characterised by coarse saddle dolomite crystals. Some bright orange luminescent spots in the dolomite most likely indicate recrystallisation of the dolomite occurred (Figures 7-17 C to E). The C4 calcite post-dating the dolomite is dull luminescent (Figures 7-17 F to H).

Mineralisation of the Cretaceous karst infill, barites, D3, C8: The C8 calcite and D3 dolomite associated with the barite mineralisation in the Cretaceous karst infill are both generally dull luminescent Figure 718 (Figures 7-18 A to D).

C9: The calcite vein cross cutting the Cretaceous karst infill is characterised by a dull- and bright luminescence similar to the C8 calcite. Calcite crystals cementing the Cretaceous karst infill can be traced into the vein (Figures 7-18 E to G, Figures 7-19 A to D). The centre of the vein C9 calcite is non- luminescent and locally bright luminescent zones can be observed (Figures 7-19 E and F).

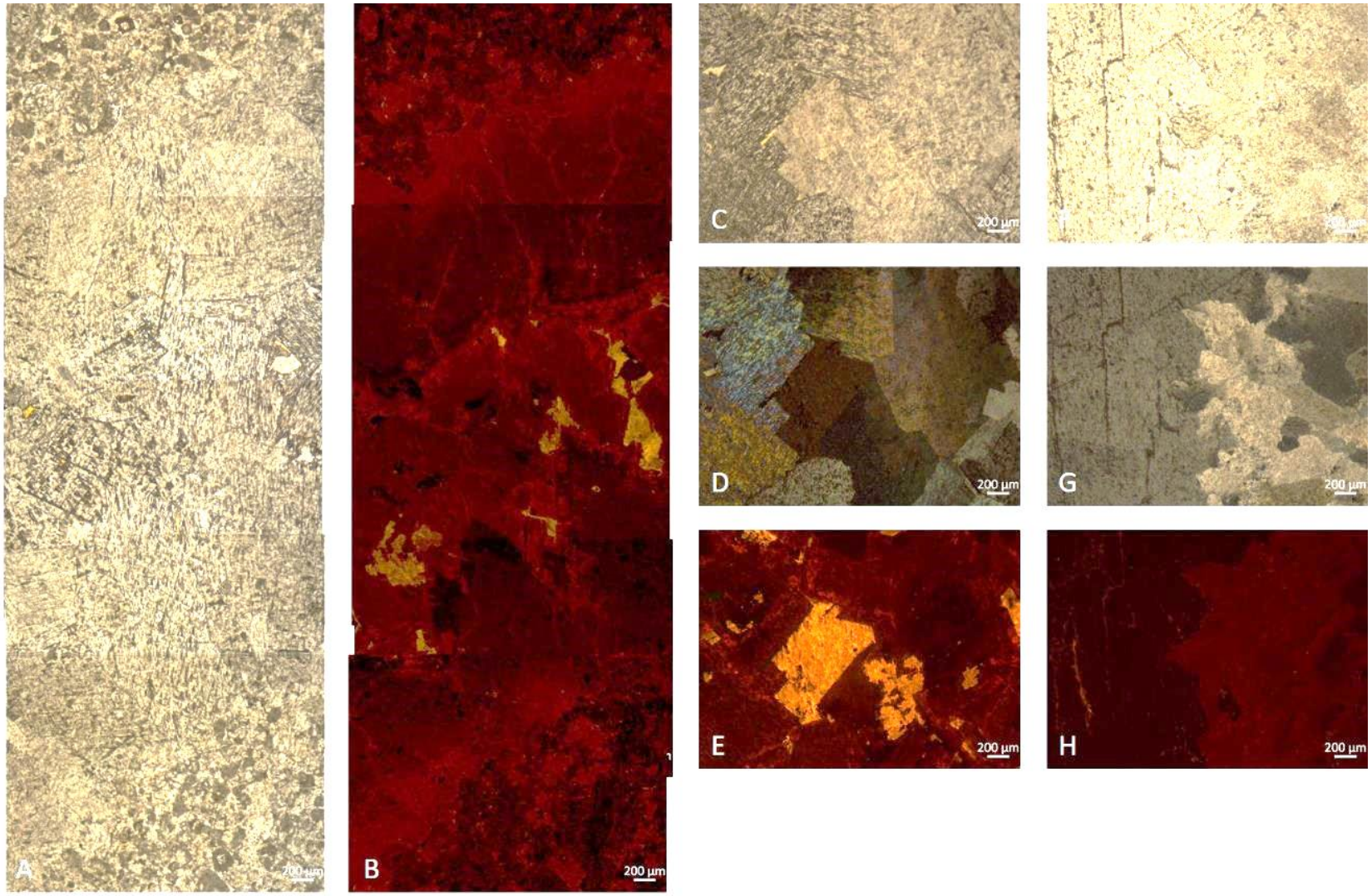

Figure 7-17: Equivalent PPL and CL microphotographs. A, B) Non and dull luminescent D2 saddle dolomite cemented vein (951.10 m). C - E) Bright orange luminescent dolomite zones probably indicate recrystallisation (951.10 m). F - H) The C4 calcite post-dating the D2 dolomite (967.77 m).

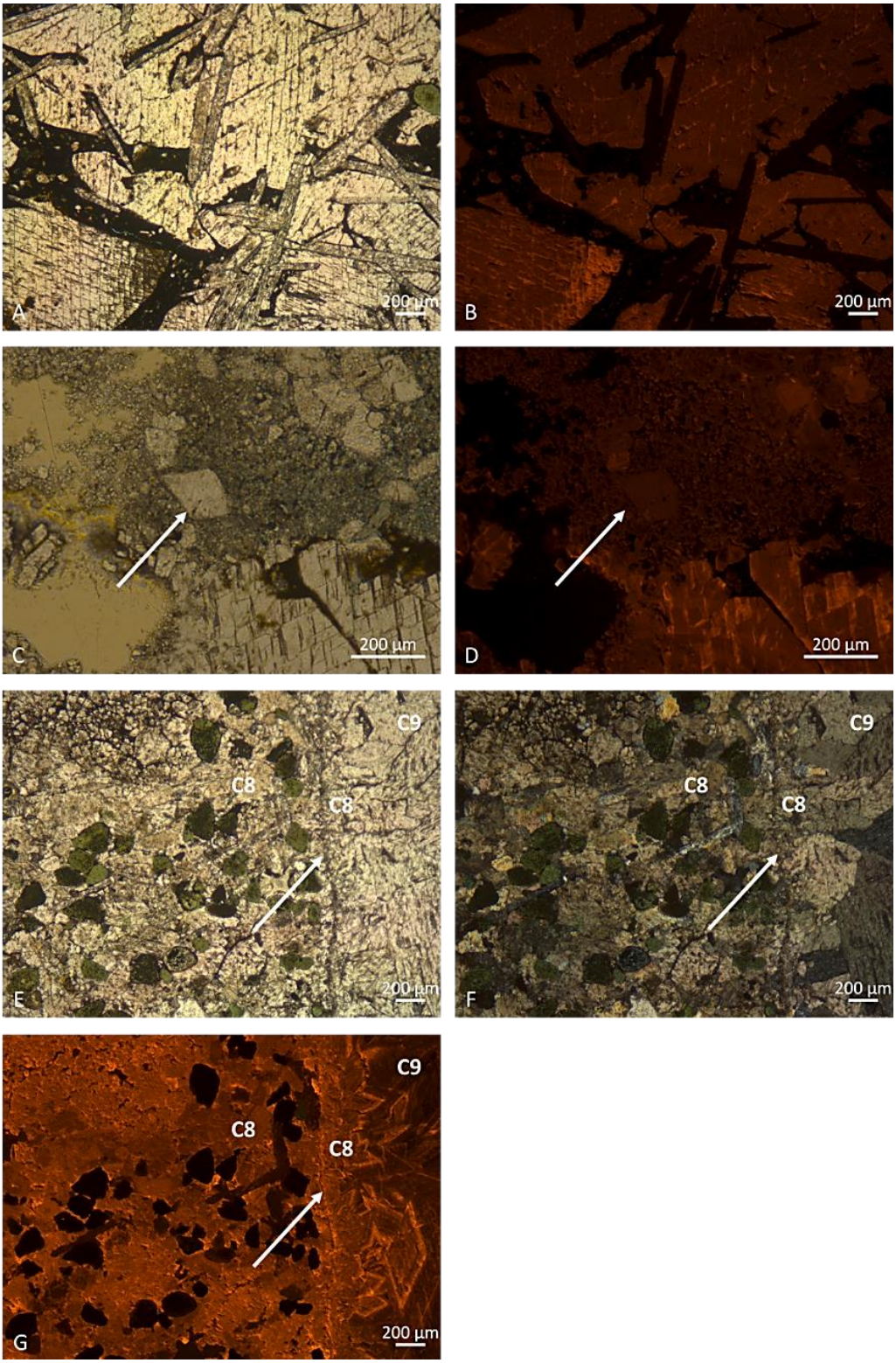

Figure 7-18: Equivalent PPL and CL microphotographs. A, B) The C8 calcite associated with the barite mineralisation of the Cretaceous karst fill is dull luminescent (976.15 m). C, D) The D3 dolomite associated with the C8 calcite is non-luminescent. E, F) Crystal boundaries of the C8 calcite cross the vein wall (white arrow) can be observed between the calcite cementing the Santonian sediments and the calcite vein. The first calcite generation in the vein also has the same luminescence as the calcite occurring within the Santonian sediment filling Cretaceous karst cavities.

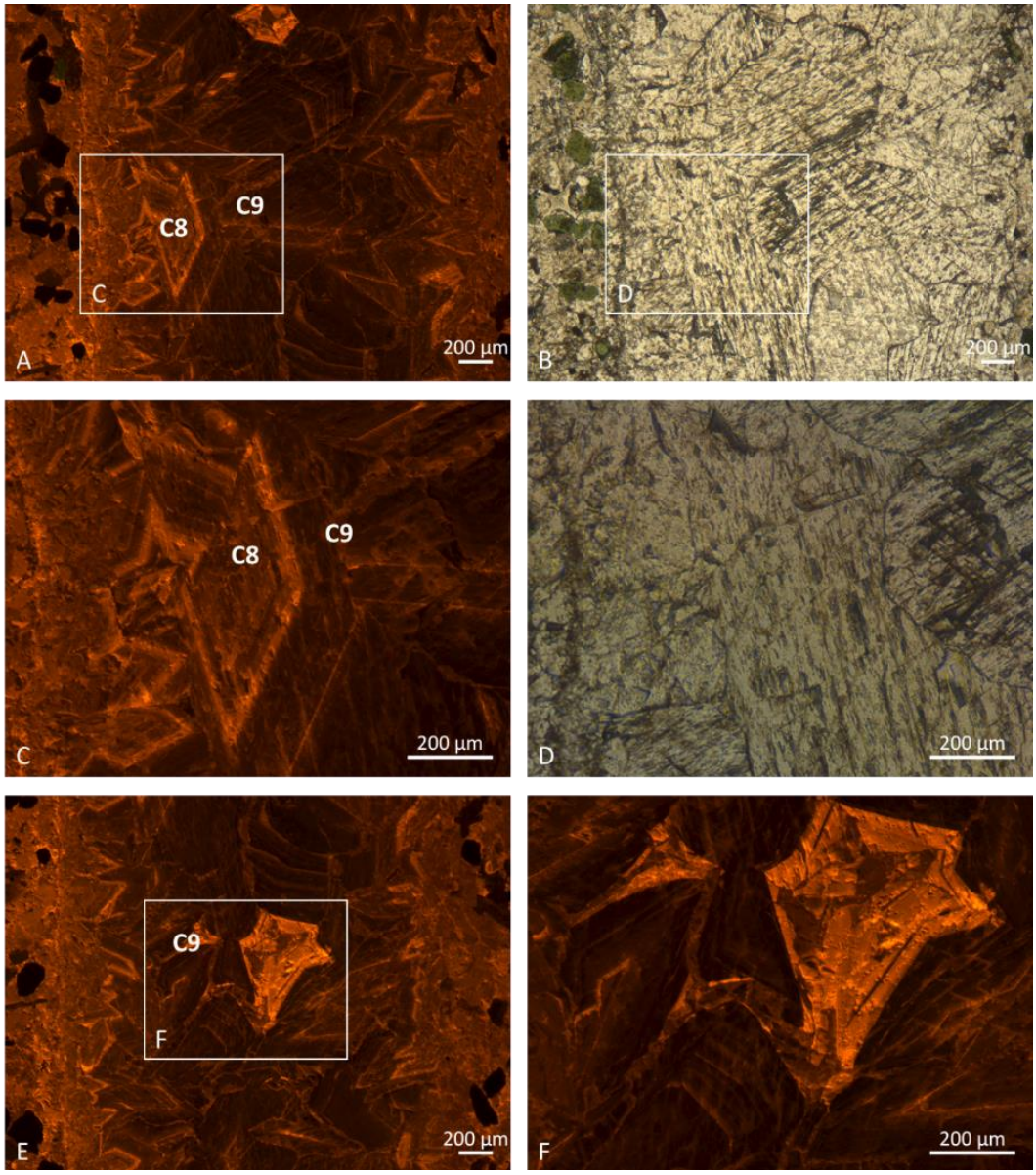

Figure 7-19: Equivalent PPL and CL microphotographs. A - D) The vein cross cutting the Cretaceous sediment is cemented by dull luminescent C8 calcite and non- and bright luminescent C9 calcite (976.75 m). E, F) Bright luminescent calcite occurs in the center of the C9 calcite vein.

7.7.3 Stable isotopes

The stable isotope results of KTG-01 (n = 18) are given in Figure 7-20. Compared to the marine reference values the oxygen isotope signature of the KTG-01 host rock (i.e. calcite matrix) is depleted, but falls within the host rock range of other wells studied.

Most of the matrix dolomite (D2) samples have a signature similar to that of the host rock of the KTG-01 and nearby BHG-01, O18-01 and S05-01. The dolomite veins (D2) have more depleted $\delta^{18}O$ values compared to the matrix dolomite samples.

The C8 calcite associate with the barites mineralisation has the most depleted $\delta^{18}O$ values, i.e. -12.13 and -14.03 ‰ VPDB. The C9 calcite cross cutting the Cretaceous karst infill is -10.38 ‰ VPDB.

Table 7-4: Stable isotope results of the KTG-01 samples expressed in per mill VPDB.

Sample (m)	Mineralogy	diagenetic phase	$\delta^{13}C$	$\delta^{18}O$
976.75	Calcite	Matrix (host rock)	1.67	-6.14
978.05	Calcite	Matrix (host rock)	2.66	-7.30
973.65	Calcite	Matrix (host rock)	2.28	-8.26
976.15	Calcite	Matrix (host rock)	2.64	-7.50
951.1	Calcite	Matrix (host rock)	2.97	-5.95
966.88	Dolomite	Matrix (D2)	3.19	-7.57
985.2	Dolomite	Matrix (D2)	4.11	-3.74
985.7	Dolomite	Matrix (D2)	4.69	-3.67
994.55	Dolomite	Matrix (D2)	3.83	-6.60
967.77	Dolomite	Matrix (D2)	3.51	-8.08
984.65	Dolomite	Matrix (D2)	3.64	-7.33
976.75	Calcite	Cretaceous karst fill	2.45	-6.75
976.15	Calcite	Cretaceous karst fill	1.80	-6.39
976.75	Calcite	Calcite vein (C9)	2.20	-10.38
984.65	Calcite	Calcite (C8)	0.96	-12.13
976.15	Calcite	Calcite (C8)	2.54	-14.03
951.1	Dolomite	Vein (D2)	2.95	-11.10
967.77	Dolomite	Vein (D2)	2.65	-10.13

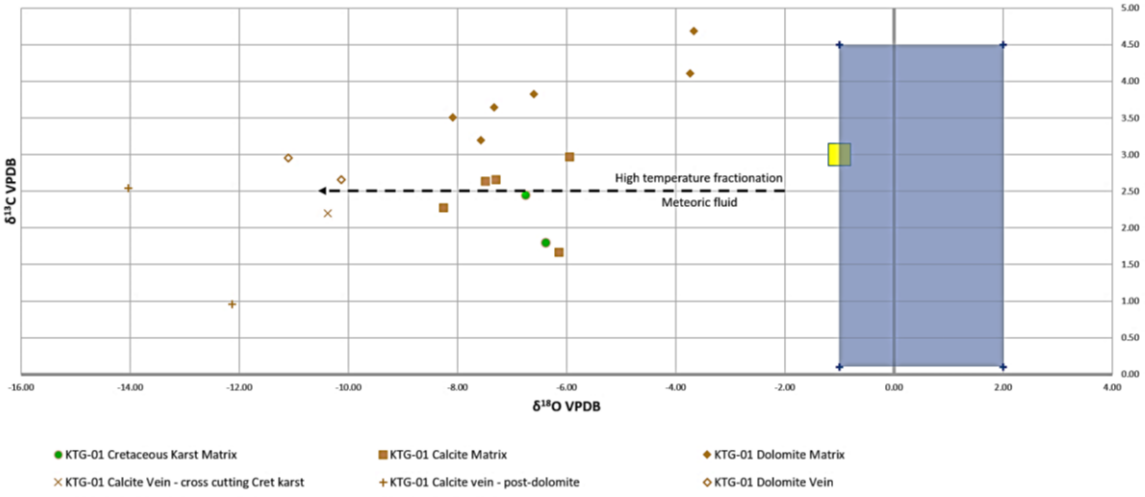

Figure 7-20: Stable isotope cross plot of the KTG-01 samples. The reference values of Dinantian marine limestones; yellow area after Muchez et al. (1991) and blue area after Nielsen et al. (1994).

7.7.4 Fluid inclusion microthermometry

D2/951.10 m: Fluid inclusion microthermometry of the D2 dolomite reveals it precipitated from a hot fluid: 69.2 °C < Th < 157.8 °C, average 133.6 °C (Figure 7-21 and Table 7-5). Many inclusions were too small for the Tm ice to be measured. The measurements the parent fluid had a wide salinity range from 1.0 to 12.1 wt. % eq. NaCl (i.e. fresh water to a brine with 4X sea water salinity). Based on the on the available data, no clear temperature - salinity

trend can be observed, but mixing of a high and a low salinity fluid cannot be excluded. The oil inclusions occur in the outer dolomite cement zone of the vein. The entrapment temperature of the oil inclusions varies between 116.8 and 151.8 °C (average: 137.0 °C).
C9/976.75 m: The calcite cementing the fracture cross cutting the Cretaceous karst infill precipitated from a low salinity (0.7-2.4 wt. % eq. NaCl), but fairly warm (72.9-122.4 °C, average: 93.4 °C) fluid (Figure 7-22 and Table 7-6).

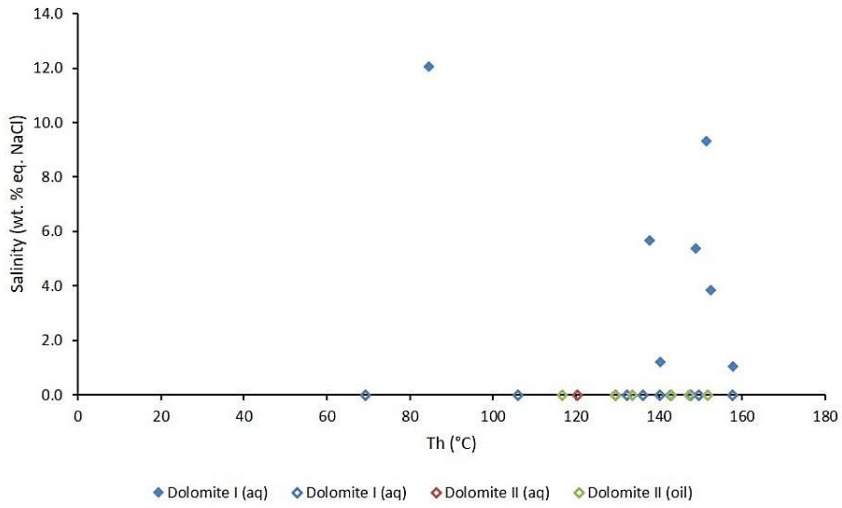

Figure 7-21: Temperature - salinity cross plot of the fluid inclusion microthermometry results of D2 dolomite (KTG-01, 951.10 m). Dolomite I refers to the dolomite cement zone without hydrocarbon inclusions. Dolomite II refers to the dolomite cement zone with hydrocarbon inclusions. Oil inclusions and inclusions which were too small for Tm ice to be measured were attributed an arbitrary salinity of 0 wt. % eq. NaCl. These data points are marked by symbols without fill.

Table 7-5: Overview of the fluid inclusion results of D2 dolomite of KTG-01, 951.10m. Dolomite I refers to the dolomite cement zone without hydrocarbon inclusions. Dolomite II refers to the dolomite cement zone with hydrocarbon inclusions. N.o. = not observed, n.a. = not applicable.

F. i. Number	F. i. Type	F. i. Host mineral	F. i. Host type	Fluorescence colour	$T_{m\,ice}$ (°C)	Salinity (wt. % $NaCl_{eq}$)	T_h (°C)
1	aq	dolomite I	primary		-0.6	1.0	157.8
2	aq	dolomite I	primary		n.o.		69.2
3	aq	dolomite I	primary		-0.7	1.2	140.4
8	aq	dolomite I	primary		n.o.		147.6
9	aq	dolomite I	primary		-3.3	5.4	148.9
10	aq	dolomite I	primary		-6.1	9.3	151.4
11	aq	dolomite I	primary		n.o.		106.1
12	aq	dolomite I	primary		-8.3	12.1	84.6
13	aq	dolomite I	primary		n.o.		142.7
14	aq	dolomite I	primary		n.o.		140.2
15	aq	dolomite I	primary		n.o.		136.1
16	aq	dolomite I	primary		n.o.		149.5
21	aq	dolomite I	primary		n.o.		157.8
22	aq	dolomite I	primary		n.o.		132.2
23	aq	dolomite I	primary		-2.3	3.8	152.5
24	aq	dolomite I	primary		-3.5	5.7	137.8
17	aq	dolomite vein II	primary		n.o.		120.4
18	aq	dolomite vein II	primary		n.o.		129.6
19	oil	dolomite vein II	primary	green-yellow	n.a.		116.8
20	oil	dolomite vein II	primary	green	n.a.		147.3
4	oil	dolomite vein II	primary	blue-green	n.a.		143.0
5	oil	dolomite vein II	primary	blue-green	n.a.		151.8
6	oil	dolomite vein II	primary	green-yellow	n.a.		133.5
7	oil	dolomite vein II	primary	green-yellow	n.a.		129.5

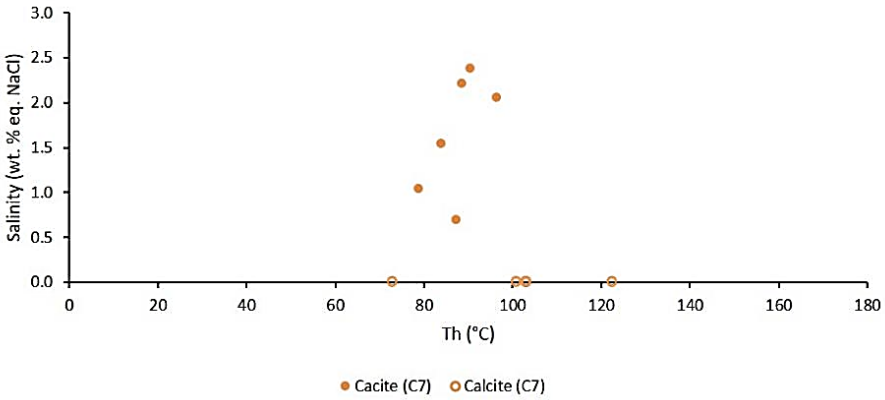

Figure 7-22: Temperature - salinity cross plot of fluid inclusion microthermometry results of the C7 calcite (KTG-01, 976.75 m). Metastable inclusions and inclusions for which Tm ice could not be observed have been were attributed an arbitrary salinity of 0 wt. % eq. NaCl. These data points are marked by symbols without fill.

Table 7-6: Overview of the fluid inclusion microthermometry results of C7 KTH-01 976.75 m. N.o. = not observed, met. = metastable

F. i. Number	F. i. Type	F. i. Host mineral	F. i. Host type	$T_{m\ ice}$ (°C)	Salinity (wt. % $NaCl_{eq}$)	T_h (°C)
1	aq	calcite	primary	n.o.		102.9
2	aq	calcite	primary	-1.4	2.4	90.3
3	aq	calcite	primary	-0.4	0.7	87.3
4	aq	calcite	primary	-0.9	1.6	83.9
5	aq	calcite	primary	-1.3	2.2	88.4
6	aq	calcite	primary	n.o.		100.9
7	aq	calcite	primary	met		103.3
8	aq	calcite	primary	met		122.4
9	aq	calcite	primary	-1.2	2.1	96.3
10	aq	calcite	primary	-0.6	1.0	78.8
11	aq	calcite	primary	met		72.9

7.7.5 Diagenetic sequence in the context of burial/thermal history

D2: The D2 dolomite precipitated from high temperature (69.2-157.8 °C, average 133.6 °C) fluids. The salinity trend (1.0-12.1 wt. % eq. NaCl) shows that mixing of a high and a low salinity fluid occurred.

The dolomite sample from KTG-01 contains two sets of cross-cutting dolomite cemented fractures, the youngest of which contains oil inclusions with yellow-green to blue-green fluorescence. The occurrence of the hydrocarbons indicates dolomitizing fluids were circulating along faults and fractures when source rocks reached the oil window. Two possible source rocks can be considered, i.e. Namurian continental deposits and Jurassic shales. The Namurian source rocks may have reached maturity during the Late Carboniferous – Early Permian. Jurassic Posidonia shales start generating hydrocarbons in the adjacent Western Netherlands Basin during the Upper Jurassic.

A clear salinity trend shows that the parent fluids of the dolomites consisted of warm brine (3.5 X sea water salinity) and low salinity (fresh water) end member. The fairly narrow temperature range indicated the fluids had similar temperatures at the time of dolomite precipitation. A meteoric freshwater end member must therefore have circulated to significant depths in the basin to warm up and reach similar temperatures as basinal brines. This restricts dolomite precipitation to periods with considerable basin inversion and exposure of lifted

blocks such as the Lower Permian (Saalian phase) and Middle-Late Jurassic to ?Upper Cretaceous. Since the dolomitisation pre-dates a Cretaceous phase of karstification, it is more likely that Late Jurassic is an optimum period for dolomitisation.
C9: The depleted $\delta^{18}O$ value and low salinity (0.7 – 2.4 wt. % eq. NaCl) indicate the C7 calcite vein cross the Cretaceous karst infill is of meteoric origin. The cathodoluminescence pattern of the C7 calcite suggests variations in the redox conditions may have occurred, however, it does not have the typical finely zoned non-bright-dull luminescence pattern of a calcite precipitated from a meteoric fluid in near surface conditions. The high temperature of the fluid (72.9 – 122.4 °C, average: 93.4 °C) also suggests precipitation under burial conditions. The minor salinity range may point towards the interaction of the meteoric fluid with country rock. The Beveland Formation has not been buried to great depth following the Cretaceous exposure and did not reach burial temperatures greater than ±50 °C. Consequently, the C9 calcite can be interpreted as the product of hydrothermally circulating meteoric water that interacts with country rock.
Depleted $\delta^{18}O$ values of host rock can be due to temperature fractionation as a consequence of HTD and mineralisation and possibly Cretaceous meteoric fluids.
Fluid inclusion microthermometry data was not acquired of the C8 calcite cement associated with the D3 dolomite and barite. It is unlikely that these diagenetic phases precipitated from a meteoric fluid. (Most mineralisations are associated with high temperature brines.) The change in cathodoluminescence from dull – bright C8 calcite to non-luminescent C9 calcite would support a change in diagenetic fluid. The depleted $\delta^{18}O$ values of the C8 calcite supports precipitation from a high temperature fluid.

7.8 Reservoir quality

Reservoir quality in the KTG-01 well is poor, with average porosity values below 1%, but with scattered values up to 26%. Matrix permeability is always low, less than 10 mD.

This page intentionally left blank

Daalsesingel 1
3511 SV Utrecht
scan@ebn.nl
www.scanaardwarmte.nl

Onderzoek in de ondergrond voor aardwarmte